Annual and Seasonal Mean Net Evaporation Rates of the Red Sea Water during Jan 1958 – Dec 2007

Sahbaldeen Abdulaziz

A thesis submitted in partial fulfillment for the degree of Master of Science in Physical Oceanography

University of Bergen
Geophysical Institute
October 2012

University of Bergen, Norway
printed version October 1, 2012

To my all family members , all who love me or been loved by me

Acknowledgements

First and foremost, words fail to express my appreciation to my supervisor Dr. Knut Barthel for the privilege of having excellent guidance and constant support during this work. I benefited a great knowledge from your supervision, enthusiasm and encouragement. You have been a wonderful supervisor. I am very grateful to you. I also thank the all staff at the Geophysical Institute for their welcoming and opened door.

I am enormously grateful to NOMA programme for providing me the financial support during my master study. Thank you for giving me the opportunity to study in Norway.

Many thanks go to the all members of The Institute of Marine Researches – Red Sea University IMR RSU for their facilities and giving hand. Many thanks go to my undergraduate study colleague Dr: Mohammad Ali who gave me his all efforts and to my friend Osama for his constant encouragement.

Last but not least, my warmest thank go to my mother Fatima and father Abdulaziz and elder brother Nasralden and my cute sisters Amani and Shosho for their constant support and prayers.

University of Bergen
Geophysical Institute

Annual and Seasonal Mean Net Evaporation Rates of the Red Sea Water during Jan 1958 – Dec 2007

Thesis for the degree of Master of Science

Abstract

Data set including sea level, temperature, salinity, and current from Simple Ocean Data Assimilation (SODA) is used in this study to estimate the mean net annually and seasonally evaporation rates. Then wind data is used to examine its impact on the evaporation. This work calculated the seasonal and annual evaporation rates based on assumption of that there is no net mass transport (balanced). Hence, the difference in the transport supposed to be equal to the water that has evaporated. Therefore data of water in-flow and out-flow used to examine the net mass transport with the obtained evaporation rate. Results revealed that the net annual mean evaporation was 1.24 m/yr and the net seasonal mean was 1.3 m/yr and the evaporation rate in winter months was permanently higher than summer and autumn with minimum value in August. The annual wind impact is masked but, it is clearer for the monthly, particularly in June and October. The monthly water exchange through Bab al-Mandeb Strait accompanied the monthly evaporation in its fluctuations with high rates of net-flow in winter and low rates in summer and exactly such as the evaporation the minimum net transport found in August. Hence, we can assume that the evaporation exerts a great influence in the Red Sea circulation.

October 2012 – Bergen, Norway,
Sahbaldeen Abdulaziz

Contents

List of figures

List of tables

Chapter 1

Introduction

1.1 Motivation

Evaporation is the major factor that determines water and salt balances of the Red Sea. The Red Sea is in a highly arid region and this makes its loss of water due to evaporation greater than its gain from precipitation and run-off. There are many previous attempts at estimating the evaporation from the various parts of the. Red SeaUsing observations collected over coastal and open waters, the reported values were calculated by different methods.

The present work is another attempt to estimate the net mean annual and seasonal rates of evaporation of the Red Sea. The data represents the time period from January 1958 to December 2007.

1.2 Site Description

The Red Sea (Al-Bahr Al-Ahmar in Arabic) is a semi-enclosed narrow sea that extends from Suez in the north at 28°N to the Bab el-Mandeb Strait in the south at 12.5°N, which connects the Red Sea with the Arabian Sea through the Gulf of Aden. It separates the coasts of Saudi Arabia and Yemen to the east in the Arabian Peninsula from those of Egypt, Sudan, and Eritrea to the west in Africa occupying an area of approximately 450,000 km^2. In north the sea splits into two narrow arms, Gulf of Suez which connects the Red Sea with the Mediterranean Sea through the Suez Canal, and Gulf of Aqaba [27]. Bab el-Mandeb shallowest section consists of Hanish Sill[1] near to Hanish Islands at about 150 km from the narrowest passage which located

[1]Data collection Area (see Chapter 3)

near to Prim Island and the sill is characterized by a total width of 110 km and depth of 137 m [41]. The Perim Narrows total width is only 18 km [19]. Figure 1.1 shows the coastline and bathymetry of the Red Sea.

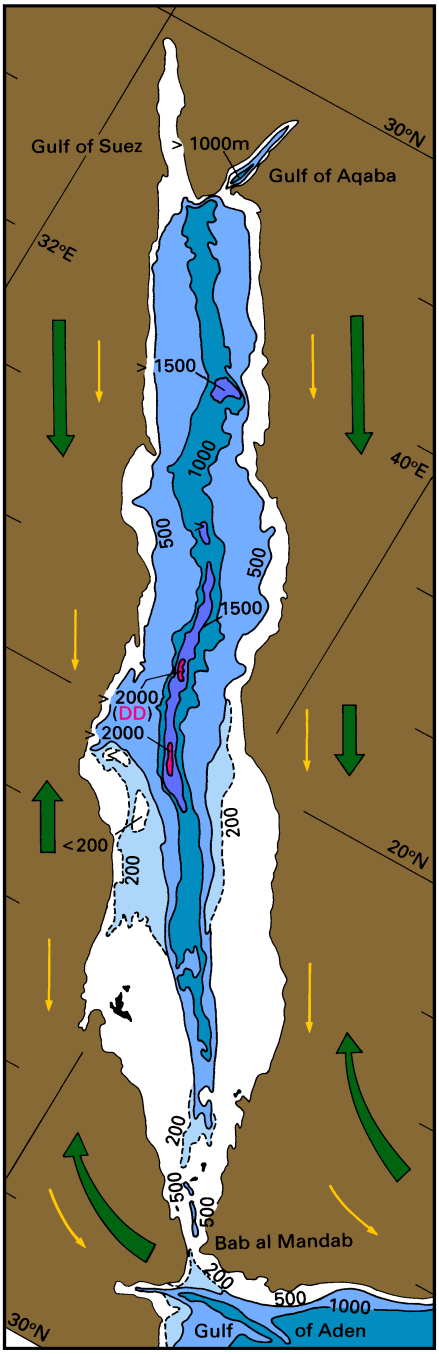

Figure 1.1: Coastline and bathymetry of the Red Sea. The arrows indicate prevalent wind directions for winter (thick arrows) and summer (thin arrows) [36].

Facts in numbers about the Red Sea, Bab el-Mandeb, Gulf of Suez and Gulf of Aqaba are mentioned by Ali [3] as it shown in Table 1.1

Table 1.1: The Red Sea and its parts in numbers, table compiled by Ali [3].

Region	The fact	Fact in number	Author
The Red Sea	Length	2000 km	Patzert [23]
	Average depth	524 km	Patzert [23]
	Average width	220 km	Patzert [23]
Gulf of Aqaba	Maximum depth	2190 m	Morcos [18]
	Length	175 km	Cochran [9]
	Depression Depths	1100 – 1400 m	Edwards [11]
Gulf of Suez	Length	300 km	Cochran [9]
	Range depth	55 – 73 m	Morcos [18]
Bab el-Mandeb Strait	Average depth	300 m	Maillard and Soliman [16]
	Narrowest width	18 km	Murray and Johns [19]
	Sill depth	137 m	Werner and Lange [41]

1.3 Physical Features

The Red Sea separates two great blocks of Earth's crust; North Africa and Arabia. Land on either side reaches heights of more than 2000 m above sea level, and the highest land is found in the south. The coastlines for a distance of about 350 km from approximately 28°N, where the Gulfs of Suez and Aqaba meet, south to latitude 25°N are quite straight and parallel to each other. Then the coastlines become more sinuous and the Red Sea gets its widest width between 16°N and 17°N [27]. Along almost the entire length of the sea there are various mountain chains (The Red Sea Mountain Chains); with some gaps on each side; and the major gap is the Tokar Gap found at about 18°N approximately 50 km from the Tokar delta on the Sudanese coast, and it is almost 110 km wide. This gap impacts on the surface wind and disturbs the along-sea winds with strong cross-sea wind [14].

1.4 The climate

The physical setting of the Red Sea area has a clear finger print on its climate. The Red Sea lies within subtropical regions, and due to this geographical position its

climate is typical desert and semi-desert which is extremely hot and arid in summer, moreover the southern part of the Red Sea is considered as one of the hottest regions in the world [38], [28].

1.4.1 Winds and Rainfall

The climate of the Red Sea results from two winds systems: the prevailing northwest winds (NNW) and the Indian monsoon system. The former all year around blows from the northwest. These winds dominate the northern part of the Red Sea particularly the regions north of 19°N [23]. These aforementioned prevailing northwest winds (NNW) are affected by the eastern Mediterranean weather systems [25]. The Indian monsoon winds control the southern part of the Red Sea south of 19°N.The winds reverse its direction from southeast (SSE) during October- May (winter); to northwest (NNW) during June – September (summer)[23]. Figure 1.2 shows the wind regimes in the Red Sea.

Water exchange between the Red Sea and the Indian Ocean is most influenced by the winds, therefore, in winter there is a surface inflow into the Red Sea because the winds blow from the southeast in the winter monsoon [35]. In summer the inflow reverses and the water flows out of the Red Sea due to the summer northwest winds [35]. Thus the wind is an important force that generates a circulation in the Red Sea and it believed to control the flow [30].

Precipitation in any form at the Red Sea region is very little therefore the fresh water input can be ignored [24]. The annual estimates of the precipitation ranging from 0.05 m/yr to 0.15 m/yr [18].

This study deals with monthly mean data of winds at the Red Sea during the time period January 1958 to December 2007, which has been analyzed and presented in chapter 3

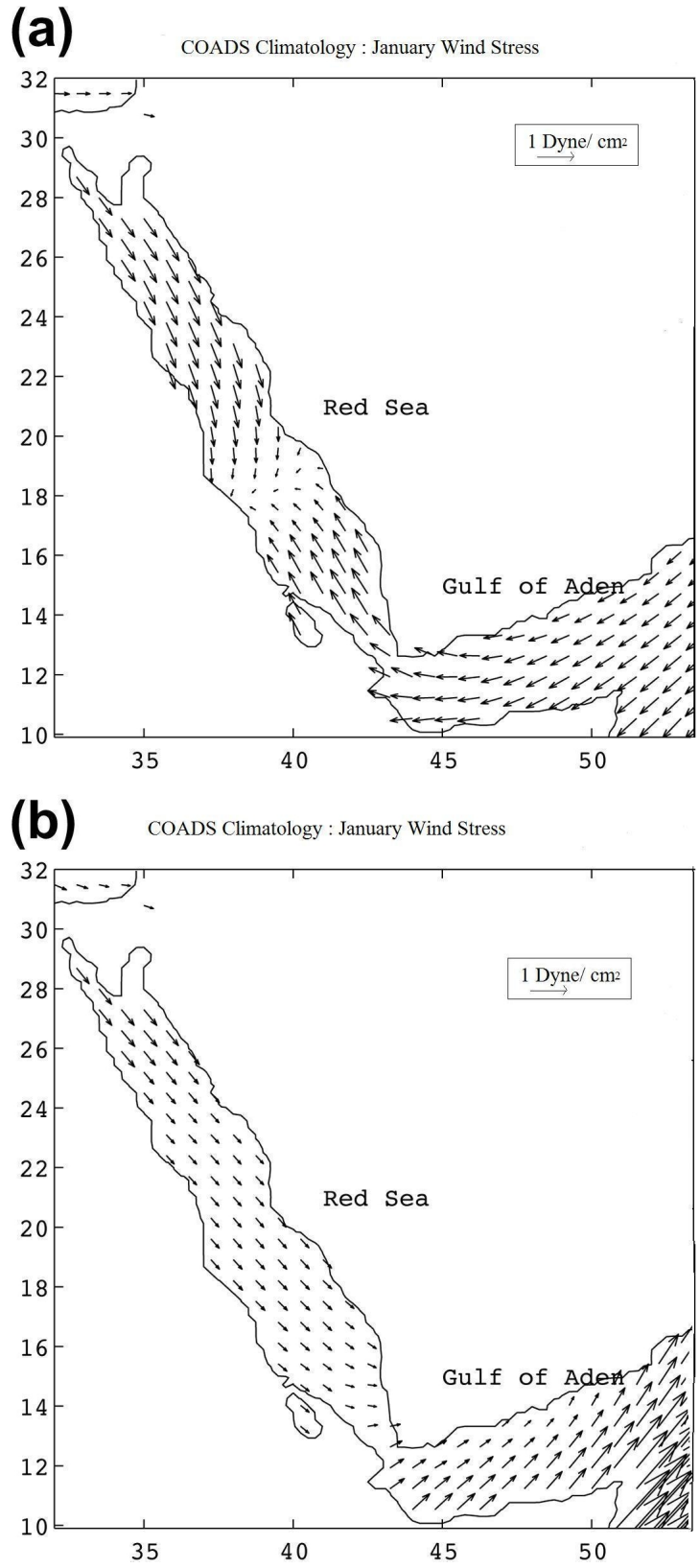

Figure 1.2: Wind stress at the Red Sea during (a) January; (b) July, from[15]

* the map in Figure1.2 has been modified from the the source map to include the Red Sea region just.

1.4.2 Salinity and Temperature

The Red Sea is believed as one of the saltiest water bodies in the world, and that is as a result of high evaporation [2] and precipitation in any form (rainfall, rivers, actually no rivers are there) is low. Figure 1.3 illustrates the annual mean surface temperature and salinity as it has been showed by Sofianos and Johns [32] study. They found that the maximum temperature is at the center, and it decreases toward the northern and the southern tip of the Red Sea. They explained the high center's temperature as a result to the very weak wind speed in the central area of the Red Sea. The salinity pattern increases from the south toward north to get its maximum in the northern end [32]. For the seasonal aspect of temperature and salinity they found that the surface temperature is very warm during the summer with a little temperature gradient toward the south as it showed in Figure 1.4b [32]. In summer the average surface temperature of the northern part of The Red Sea is approximately 26°C, whilst, it is 30°C in the southern part [29]. The highest temperature during winter is found at the eastern boundary particularly at the southern and central Red Sea eastern boundary (Figure 1.4a), while it is lower during summer at the same eastern boundary. This difference of temperature is related to the prevailing wind which leads to coastal upwelling during the summer and coastal downwelling during the winter along the eastern boundary in the southern part [32]. The temperature at the northern and the southern parts varies by approximately 2°C during the winter from aforementioned values for the two parts during the summer and the overall water temperature is averaged by 22°C [29].

The effect of the summer coastal upwelling influences in the salinity distribution, that Sofianos and Johns [32] observed fresh water over the eastern boundary. They meant that the fresh water as a result of upwelling of the GAIW which enters the Red sea during the summer [32]. The salinity increases from the south (36.0) toward the north(>40.1); it is low in the south due to Gulf Aden recharges, and high in the north due to high evaporation and Gulf of Suez water discharge [29]. The salinity distribution is shown in (Figure 1.5 c and d).

[2] The main issue of this study

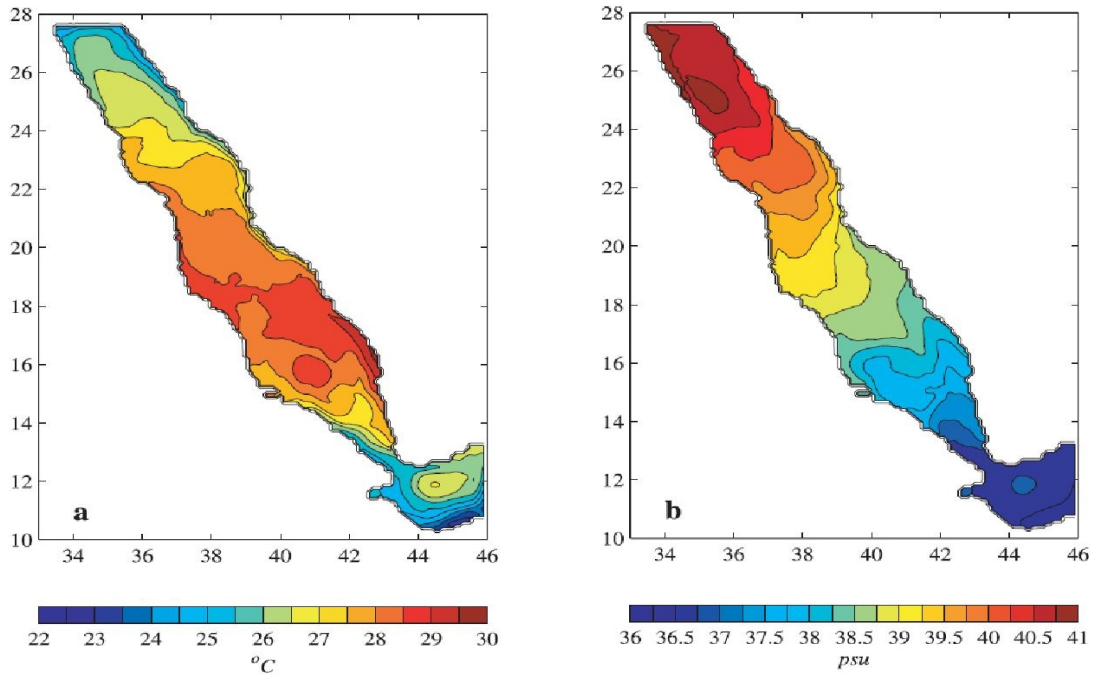

Figure 1.3: The Red Sea annual mean (a) sea surface temperature (b) salinity from MICOM simulation, from [32]

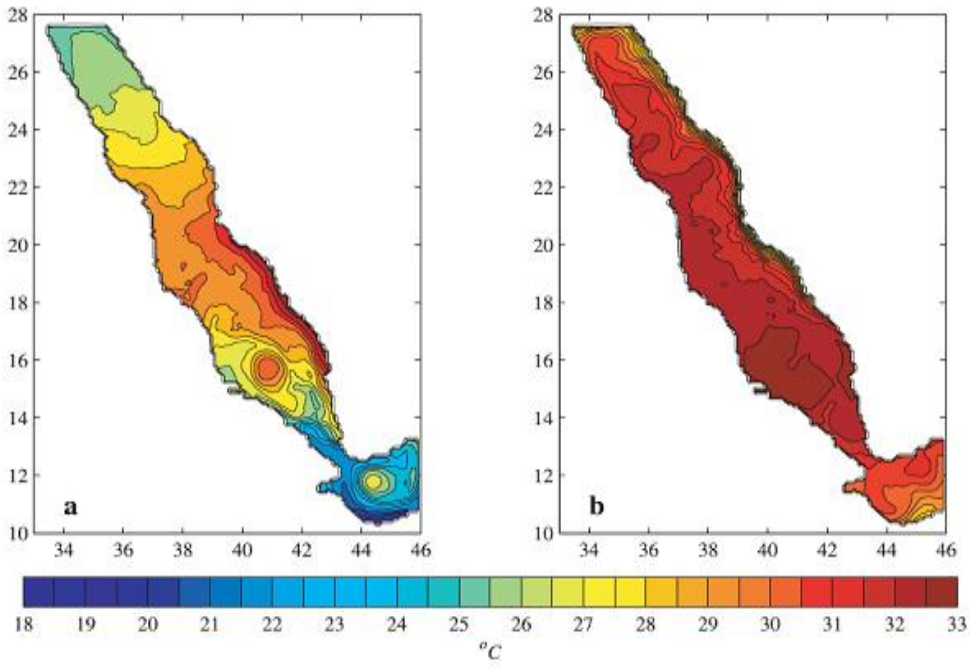

Figure 1.4: Distribution of the seasonal sea surface temperature at the Red Sea during: (a) winter (November-March) and (b) summer (June-September) from [32].

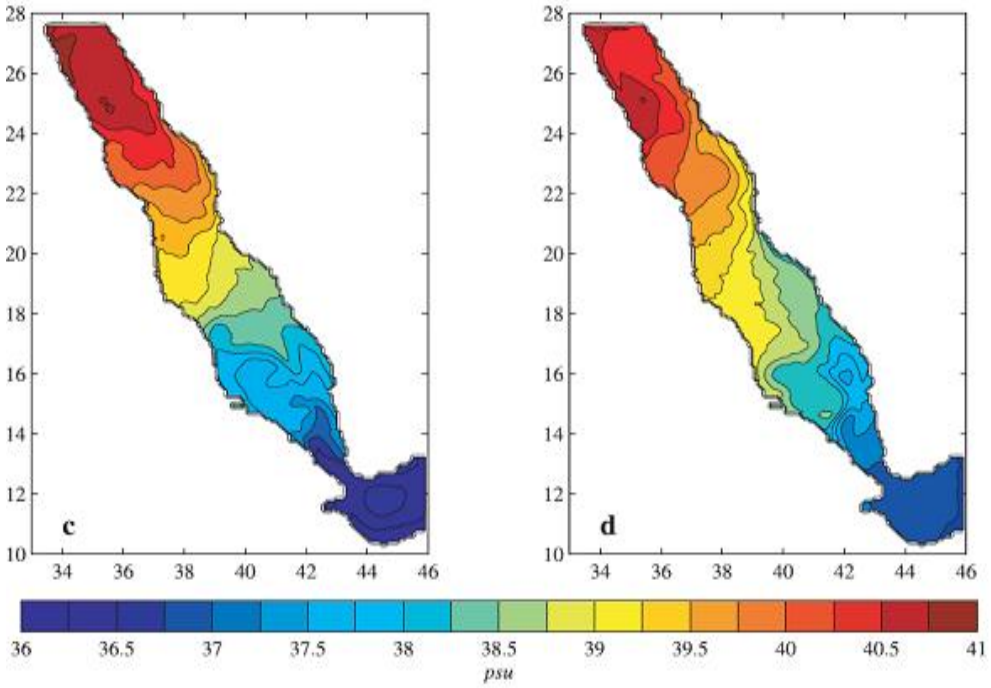

Figure 1.5: Distribution of the seasonal sea surface Salinty at the Red Sea during:(c) Winter (November-March) and (d) summer (June-September) from [32].

1.5 Water Masses and Exchanges with Adjacent Seas

The mass exchange through Bab el-Mandeb has been studied by Smeed[31] The Red Sea has only one connection to the global oceans which is the Bab el-Mandeb Strait, despite the Red Sea connects with the Mediterranean Sea through Suez Canal, but this Canal does not allow a significant flux between the two seas. The notable phenomenon is the seasonal variability of the flow at the Bab el-Mandeb as a consequence of monsoon climate there. From October to May (the winter season regime) there is an exchange of two layers: the inflow of the fresh, Gulf of Aden warmer Surface Water (GASW) entering the Red Sea in the surface layer and the Red Sea saltier and cooler outflow water entering into the Gulf of Aden in the lower layer (Figure1.6a). In the summer it is quite different. Hence, there is an exchange of three layers: the surface inflow of the Gulf of Aden surface water (GASW) reversed to flow out of the Red Sea in the surface layer, the outflow of the high-salinity Red Sea water is reduced but still remains, and between these two outflow layers there is a new layer with inflow of

cool and fresh Gulf of Aden Intermediate Water (GAIW), (Figure 1.6b). This is the winter and summer exchanges as it discussed by [31].

Evaporation rate over the Red Sea exceeds precipitation by about 2 m/yr [18]. This leads to form very high salty waters [3] and it is believed that the formation of this dense water due to the high evaporation has a great importance in the circulation of the Red Sea [20]. The wind also, as mentioned before plays a main role in the circulation and it governs the flow [30].

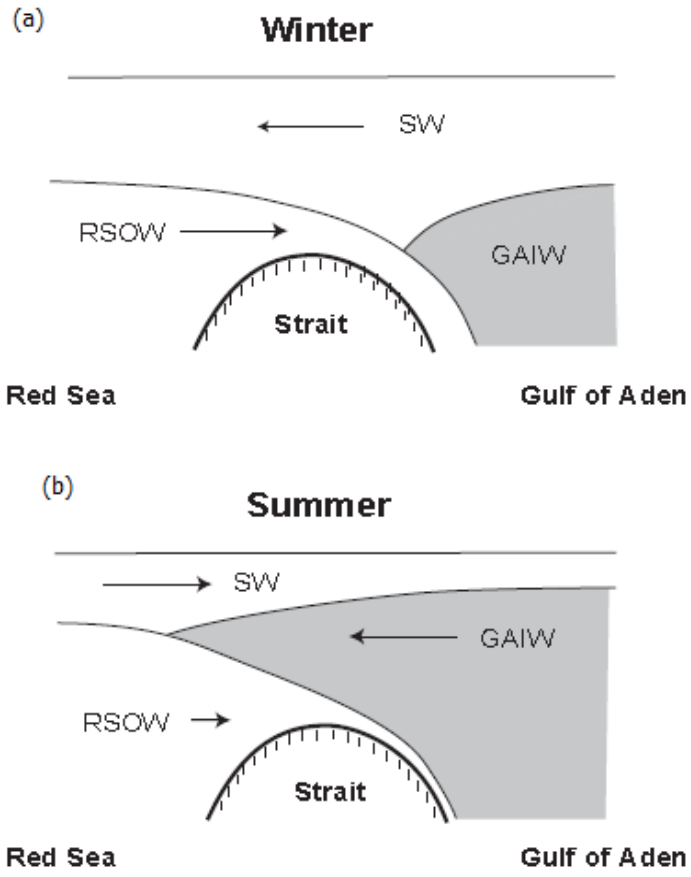

Figure 1.6: The two vertical circulations of water in the Bab el-Mandeb. (a) Winter (b) Summer. SW=Surface Water, GAIW = Gulf of Aden Intermediate Water and RSOW=Red Sea Outflow Water, from [31].

[3] Salinity exceeds 40

1.6 Currents

The Red Sea surface circulation has been investigated by Sofiano and Johns (2003) [32] using the Miami Isopycnic Coordinate Ocean Model (MICOM). They noted that the main current characteristics in the south are a mesoscale gyre which reverses its rotation from a cyclonic rotation during the summer to an anticyclonic rotation during the winter. In the peak of the winter it achieves greater than 0.5 m/s of current velocities. They also noted that during the winter there is a strong inflow in the Strait of Bab el-Mandeb and after the flow entered the basin it makes an intensive northward western boundary current. The velocity of this boundary current is greater than 20 cm/s and its velocity depend upon the inflow intensity. This western boundary current flows about 400 km into the Red Sea(till abou 16°N); then it leaves the coast and crosses to the eastern side and continues as an intensive boundary current along the eastern coast of the Red Sea (Figure 1.7). This northward western boundary current is not observed during the summer in the southern part of the Red Sea (Figure 1.8) [32].

As a result of high evaporation in the north of the Red Sea the salinity increases and the surface water temperature decreases. These two processes contribute to increase the density, thereby; the surface water sinks to the lower and deep layers [23]. Hence, a northward sea surface tilt is formed as a consequence of this mechanism. Therefore, the upper layer flows northward against the wind [23]. In winter the currents are directed to the north in the southern region due to the south-easterly winds. The surface current is directed to the south in summer flowing out of the Strait of Bab al- Mandeb due to the north-westerly winds which dominate the entire Red Sea, and due to the lower sea level in the Gulf of Aden [23].

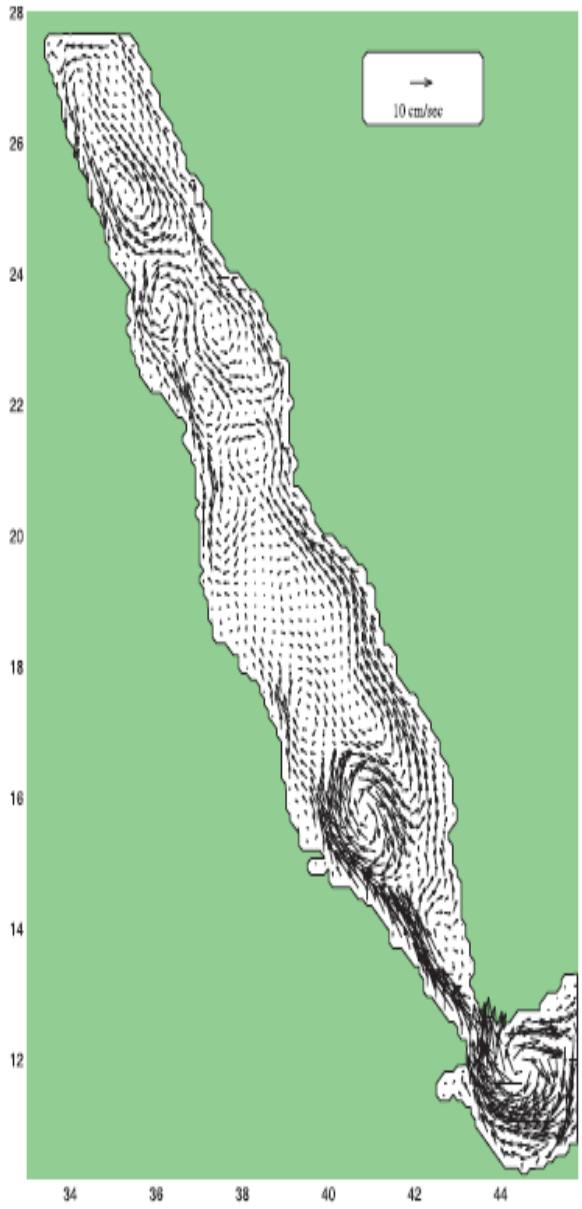

Figure 1.7: Mean surface circulation in the winter, from MICOM simulation [32].

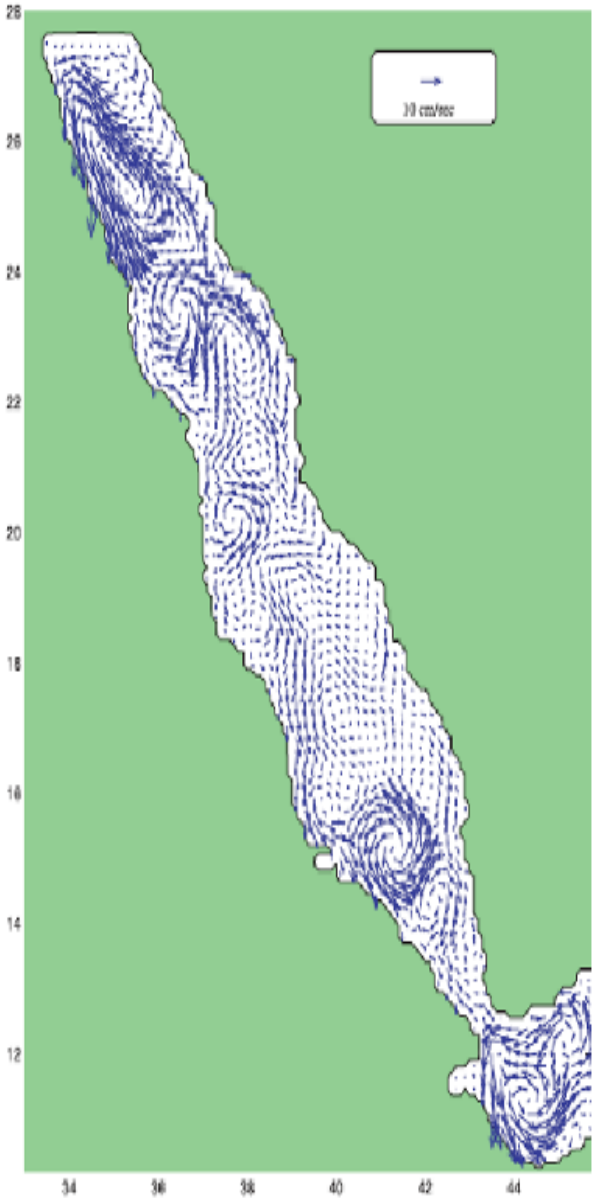

Figure 1.8: Mean surface circulation in the summer, from MICOM simulation [32].

Chapter 2

Introduction to Evaporation

Evaporation Evaporation is defined as the process by which the liquid form of water is converted to water vapor (vaporization) and removed from the evaporating surface (vapor removal) to the atmosphere. The water evaporates from a variety of surfaces, such as lakes, rivers, land surface and oceans, and the last one is considered as the source which delivers 80% of the water that is delivered by the precipitation [17].

In this chapter we attempt to give a brief definition of the process of evaporation and mention factors that affect upon it. Also we mention some previous studies and estimations of the evaporation rates at the Red Sea.

2.1 The Sea Water Evaporation

The sea water evaporation is an important aspect of sea-air interaction. Investigation of the observed variation of evaporation requires examining the weather's forcing parameters that affect upon the evaporation rate such as: air temperature, wind speed and humidity. When water temperature increases, and the wind makes the air humidity drop, then the evaporation rate reaches high values [17]. Figure 2.1 illustrates the three weather parameters that affect on the evaporation rate.

2.1.1 Evaporation and Temperature

Evaporation occurs at all the time, and at any temperature. At the water's surface; water molecules are always moving, when the water temperature increases the molecules of the water gain more energy to move faster, and this rapid movement make the water molecules able to escape to the atmosphere. Hence, any increase in

the water temperature leads directly to increase the evaporation of that water [40].

The Red Sea Region is one of the hottest in the whole world thus, it is expected that the temperature significantly impacts on the evaporation of the area.

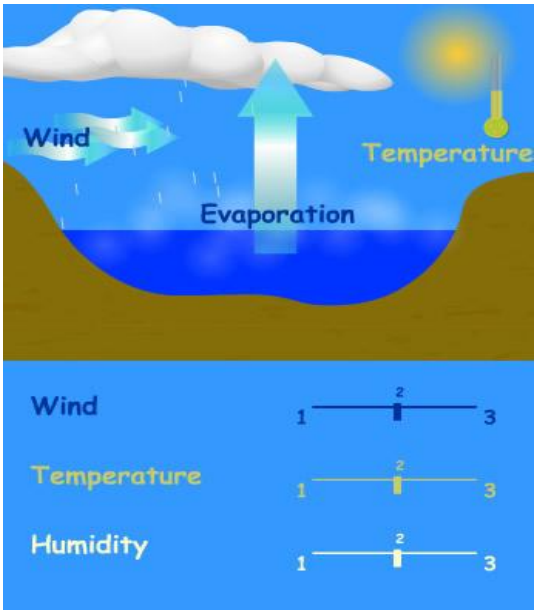

Figure 2.1: Parameters that affect on the sea evaporation rate, from [17].

2.1.2 Evaporation and Winds

The wind has two important characteristics: speed and direction. It is known that when we assume the other meteorological factors that effect on the evaporation rate as constant then, any change in the wind speed affects and causes the change in evaporation rate [12]. The wind removes the water vapour above the water's surface the reason which gives space for more water's molecules to escape into the atmosphere thus, the wind rises the rate of the evaporation and we can say there is a positive relationship between them, thus, the stronger the wind, the higher rate of the evaporation [40].

2.1.3 Evaporation and Humidity

The amount of water vapor in the air refers to air humidity, and it should be lower than the humidity of the evaporating sea surface for evaporation to occur. Turbulent air movement associated to surface roughness and wind speed gives much facility for the evaporation process that the wind carries water vapor away from the evaporating surface and thus it helps to conserve a vertical air-sea humidity gradient [44]. Thus we can say there is a negative relationship between the air humidity and the evaporation rate, the higher humidity, the lower the rate of evaporation and vice versa.

2.2 Evaporation and the Sea Level

The Red Sea is very sensitive to the sea level change because it has only one entrance to the world oceans (Bab al-Mandeb). Its level is mostly influenced by the wind stress effect and the joint effect of evaporation and the exchange of the water through the Strait of Bab el-Mandeb [34]. In spite of that the evaporation of the Red Sea is high in winter [26]; almost all previous investigations which were concerned with the seasonal changes in the Red Sea level consensually led to the reality that sea level is high in winter and low in summer Edwards 1987 [11], Morcos 1970 [18], Osman 1985 [22] and Sultan 1995 [34].

2.3 Previous Studies

There are no rivers discharging into the basin and the runoff is negligible as it mentioned before the precipitation is small. The evaporation rate of the Red Sea water is believed to be the highest rate in the whole world ocean, but there are considerable differences in annual mean value as well as seasonal cycle among the available estimates. Vercelli [39] is the first person who attempted to determine the evaporation. He used pan measurements aboard a ship and on the coast. He estimated a value of 3.5 m yr^{-1} and that was quite high and a doubtful value [33]. and that was quite high and a doubtful value. Then, several investigators followed Vercelli attempt to estimate the evaporation rate for the Red Sea water. All later estimations are showed by Sofianos et al. (2002) are given in Table 2.1 from [33].

Table 2.1: Available evaporation rate estimates for the Red Sea, from [33].

Author	Date	Evaporation estimated value m/yr
Vercelli [39]	1925	3.5
Yegorov [43]	1950	2.3
Neumann [21]	1952	2.15
Wüst [42]	1954	1.925
Privett [26]	1959	1.83
Bogdanova [4]	1974	2.66
Morcos [18]	1970	2.1
Hastenrath and Lamb [13]	1979	1.54
Bunker et al. [5]	1982	2.3
Ahmad and Sultan [1]	1987	2.07
Ahmed and Sultan [2]	1989	2.13
Osman [22]	1985	2.04
da Silva et al. [10]	1994	1.5
Tragou et al. [37]	1999	1.75

Chapter 3

Data and Methods

3.1 Data collection region

The data of this study has been collected for the vertical section at the Hanish Sill 13.25°N. As it mentioned in chapter one (Introduction); the Red Sea connected with the Gulf of Aden through Bab el-Mandeb Strait. At 150km to the north of the narrowest passage (Perim Narrows) Hanish Sill which is the shallowest section of Bab el-Mandeb Strait is located with following characteristics:

Table 3.1: Hanish Sill characteristics.

Fact	Fact in Number	Author
The deepest depth at the Sill	137 m	[41]
The total width of the Sill section	110 km	[41]
The total width at Perim Narrows	18 km	[19]

3.2 The Simple Ocean Data Assimilation Dataset (SODA)

The SODA data are model forecast produced by an ocean general circulation model. In SODA the direct observationsis is used to correct the model errors in order to improve the reanalysis of ocean variables [6].

Depending on the experiment setup, there are numerous versions of SODA [7]. Version 2.0.4, which used in this study, replaced SODA 2.0.3 and spans from January 1958 to December 2007.

From the SODA dataset we have selected the northward current component, salinity, temperature, and sea level from the Hanish sill (13.25°N) covering the whole time period January 1958 – December 2007. In addition we used the windstress for the whole Red Sea. The data were used in order to estimate the variability of evaporation of the Red Sea during the 50 years period. We hence dealt with six hundred monthly mean values of current velocity, temperature, and salinity at five longitudes and eleven layers (see Figure 3.1) covering the fifty year period.

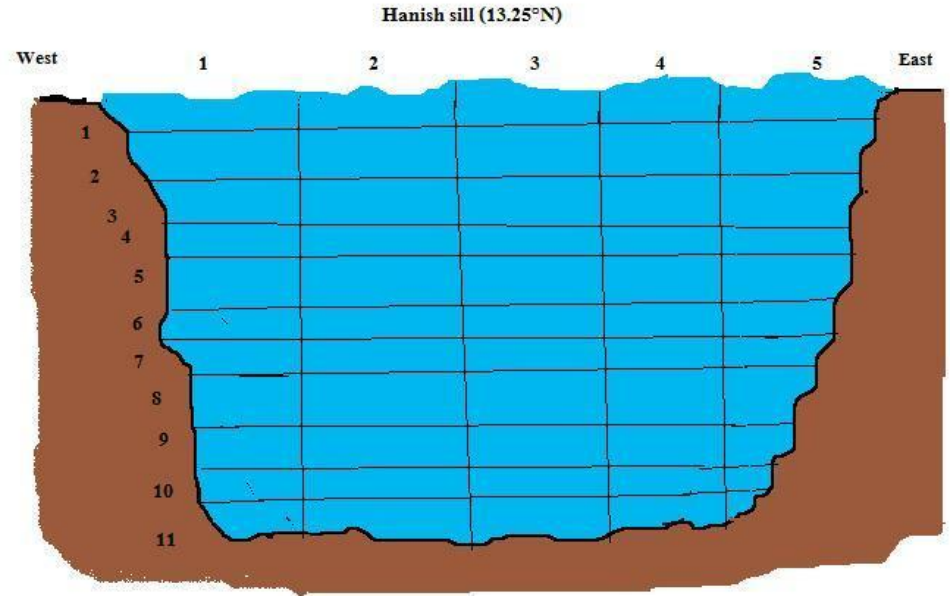

Figure 3.1: Cross section for Hanish Sill (13.25°N).

3.2.1 The Reanalysis System

The SODA reanalysis project is a multi-institutional shared project. Since it began in the mid-1990s at the University of Maryland; it keeps giving a continuous effort to improve the oceanic reanalysis. The average horizontal resolution is $0.25° \times 0.4°$ of longitude and latitude, and 40 vertical levels. The forecasts are continuously corrected by observations [6]

This kind of model plus observational data are called reanalysis; So SODA reanalysis data is a combination of model result and observation. Observations are irregularly spread over the world ocean, and also with gaps in time. When combined with model forecast we get a regular grid of data with no gaps in time.

3.3 The Method

The Evaporation rate derived from the salt flux at Hanish sill is based on the equations descibed in following Sections

3.3.1 Salt budget

We assume there is no net transport of salt, that is:

$$\iint \rho(x,z)S(x,z)V(x,z)dxdz = 0. \tag{3.1}$$

The double integration is approximated by the double sum,

$$\Delta x \sum_{i=1}^{5}\sum_{j=1}^{11} \rho(i,j)S(i,j)V(i,j)\Delta z(i,j) = 0, \tag{3.2}$$

Where the width of each cell is $\Delta x =$ constant and:

$\rho \equiv$the density

$S \equiv$the salinity

$V \equiv$the velocity

$\Delta z \equiv$the layer thickness, eleven thicknesses that increase with depth. The upper ten have the standard values: 10 m, 10 m, 10 m, 11 m, 11 m, 12 m, 12 m, 13 m, 15 m and 16 m, which span a depth of 120 m.

The SODA data do not have information on the actual thickness of the bottom cell therefore we used a minimization method to find the five cells thicknesses at the Hanish sill. The method was to calculate the net salt flux through the vertical section, which should be equal to zero, and choose that combination of the five thicknesses which gave the least net salt flux. This was: 12 m, 14 m, 13 m, 16 m, 9 m.

3.3.2 Mass budget

We assume there is no net transport of water, that is:

$$P + R - E + \iint \rho(x,z)V(x,z)dxdz = 0, \tag{3.3}$$

where:

$P \equiv$Precipitation

$R \equiv$River input

$E \equiv$Evaporation

Equation 3.3 can be approximated by the double sum,

$$P + R - E + \Delta x \sum_{i=1}^{5} \sum_{j=1}^{11} \rho(i,j) V(i,j) \Delta z(i,j) = 0. \tag{3.4}$$

From Equation (3.4) we could immediately estimate $E - P$ (assuming $R = 0$ for the Red Sea), but it is better to calculate the evaporation rate from the salt flux because if it is calculated from the formula $E - P = \sum \rho V \Delta x \Delta z$ the result will be very inaccurate, because the difference of two large numbers gives high inaccuracy. Then we can calculate the mean cross section salinity from:

$$\overline{S} = \frac{\iint S(x,z) dx dz}{\iint dx dz}, \tag{3.5}$$

This can be approximated by:

$$\overline{S} = \frac{\sum_{i=1}^{5} \sum_{j=1}^{11} S(i,j) \Delta z(i,j)}{\sum_{i=1}^{5} \sum_{j=1}^{11} \Delta z(i,j)}. \tag{3.6}$$

The deviation of salinity is:

$$S' = S(x,z) - \overline{S}. \tag{3.7}$$

From (3.1) and (3.7), we have

$$\begin{aligned} \iint \rho \left(S' + \overline{S} \right) V(x,z) dx dz &= 0, \\ \overline{S} \iint \rho V dx dz + \iint \rho S' V dx dz &= 0, \end{aligned} \tag{3.8}$$

From (3.3)

$$\iint \rho V dxdz = -(P - E + R)$$

Insert in (3.8)

$$\overline{S}\left[-(P + R - E)\right] + \iint \rho S' V dxdz = 0,$$

$$(P + R - E) = \frac{\iint \rho S' V dxdz}{\overline{S}}. \tag{3.9}$$

We assume that $R = 0$, then the evaporation is:

$$E = P - \frac{\iint \rho S' V dxdz}{\overline{S}}. \tag{3.10}$$

The unit in equation (3.10) is [kg /s], which can be transferred to meter per year as

$$E_{myr} = \frac{E \times SPD \times DPY}{\rho f \times A}, \tag{3.11}$$

Where ρf is the fresh water density, and A is the Red Sea area, SPD is seconds per day and DPY is days per year.

Equation (3.10) can be approximated as:

$$E = P - \frac{\Delta x}{\overline{S}} \sum_{i=1}^{5} \sum_{j=1}^{11} \rho(i,j) S'(i,j) V(i,j) \Delta z(i,j). \tag{3.12}$$

3.4 Leakage Term

The previous equations neglected the reality of that the sea level is changing (particularly from season to season); so the mass flux may considered as conserved while it is not like so. For example there may be a positive netflow (inflow > outflow) and this netflow may lead to rise the sea level so it will be consumed and Vice versa. Hence, it will appear as the mass flux is conserved and there is no net transport when, there is some flux is consumed and disappeared. Thus, to get more accurate estimate for the evaporation based on our assumption of there is no net flow we should add the leakage term.

From Equation (3.7) the salt budget including leakage term becomes

$$\iint \rho \left(S' + \overline{S}\right) V(x,z) dxdz = S_i A \rho_s \frac{\Delta\eta}{\Delta t}. \tag{3.13}$$

Where:

$S_i \equiv$ Salinity of leakage.

$\rho_s \equiv$Density of leakage.

$\frac{\Delta\eta}{\Delta t} \equiv$Rate of sea level change of the Red Sea.

$t \equiv$1 month.

$A \equiv$Red Sea Area.

The salt leakage term, T_i^s in Equation (3.13):

$$\overline{S} \iint \rho V dxdz + \iint \rho S' V dxdz = T_i^S. \tag{3.14}$$

Similarity the mass budget equation with leakage becomes:

$$\iint \rho V dxdz = -(P + R - E) + T_i^M. \tag{3.15}$$

Where:

$T_i^M \equiv$Mass Leakage.

Next we assume that: Salt Leakage=Salinity of Leakage water×Mass Leakage.

$$T_i^S = S_i T_i^M. \tag{3.16}$$

Insert (3.15) in (3.14)

$$\overline{S}\left[-(P + R - E)\right] + \overline{S} T_i^M + \iint S' \rho V dxdz = T_i^S.$$

Then:

$$\begin{aligned}(P + R - E) &= \frac{1}{\overline{S}} \iint \rho S' V dxdz + T_i^M + \frac{S_i T_i^M}{\overline{S}}, \\ (P + R - E) &= \frac{1}{\overline{S}} \iint \rho S' V dxdz + \underbrace{\frac{T_i^M}{\overline{S}} \left(\overline{S} - S_i\right)}_{\text{Leakage Term}}.\end{aligned} \tag{3.17}$$

The surface height of Hanish Sill is known and it added for the fives surface layers. So here we assumed the leakage is in the bottom layer.

Chapter 4

Results and Discussion

4.1 Time Series of the Evaporation

Figure 4.1 presents time series of the net annual mean evaporation for the Red Sea for time period January 1958 to December 2007. The highest obtained value is 1.88 m/yr during 1972, and the lowest value is 0.8 m/yr during 1974 and the mean annual net evaporation from the Red Sea is 1.24 m/yr. This value is a little bit larger than 1.1 m/yr, the net annual evaporation value (evaporation minus precipitation) estimated by [8]. After adding the estimated annual precipitation of 0.15m/yr we get a mean annual evaporation rate of 1.39 m/yr. This value is a bit less than 1.8 m/yr the value which has been estimated by [26]. Different previously estimated values of the evaporation from the Red Sea have been listed in Table 2.1. From the figure it is clear that the evaporation rate decreased in the recent years from 2001to 2007 and there were no notable fluctuations and variations from year to year through that period. The value estimated in this study is about 0.5 m/yr less than most other estimates. The the coarse resolution of the SODA model grid at Hanish sill may influence in the result. Another reason may be the rather weak windstresses used by SODA.

Figure 4.2 presents the mean seasonal (monthly) net evaporation for the Red Sea. The highest seasonal evaporation is in April (late winter) with 1.98 m/yr, and the lowest is in August with approximately 0.2 m/yr and the mean seasonal net evaporation is 1.30 m/yr. This result is in accordance with [37] who illustrated (in their Figure 8a) the latent heat loss of the Red Sea during the year. It showed that the latent heat loss is least during summer. This means evaporation is least during summer.

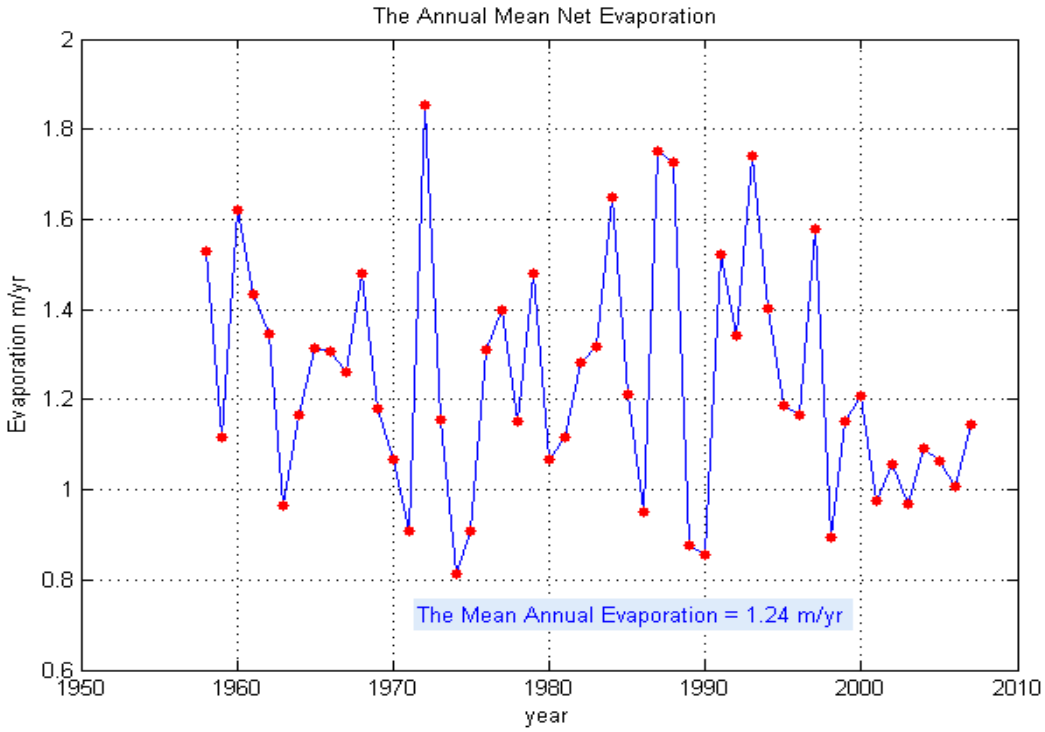

Figure 4.1: The mean annual net evaporation in the Red Sea.

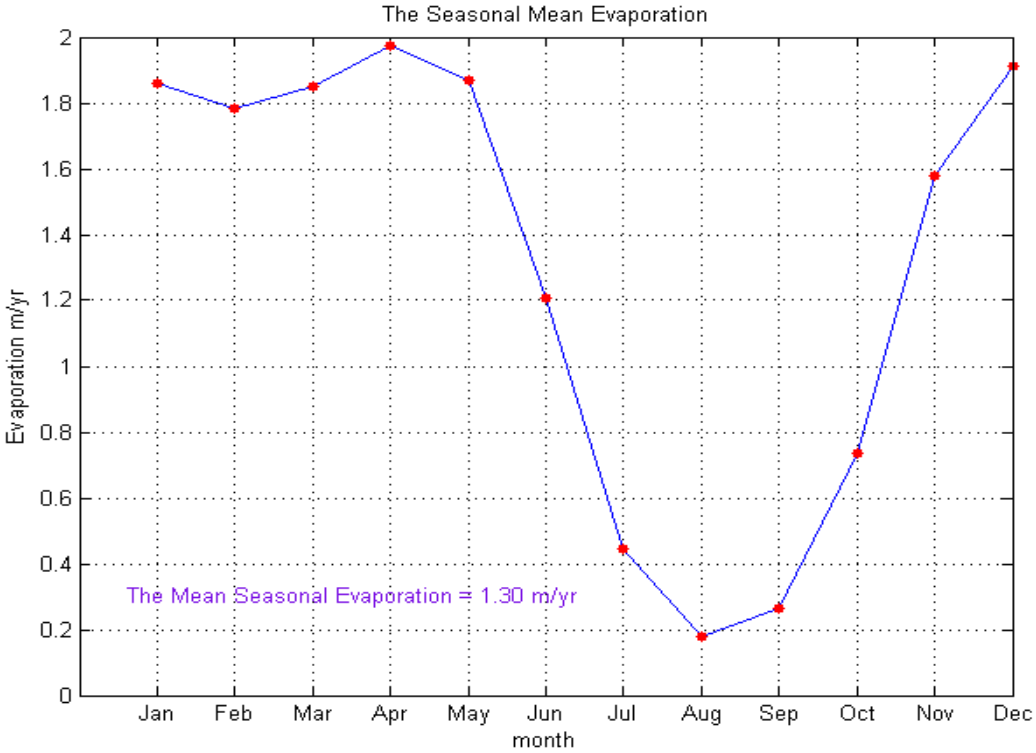

Figure 4.2: Monthly net evaporation in the Red Sea.

Figure 4.3 presents the seasonal mean net evaporation (blue curve) and the seasonal mean net evaporation after added the leakage term (red curve)The noticeable thing is that there is no great difference between the two curves therefore the leakage term can be neglected in this study.

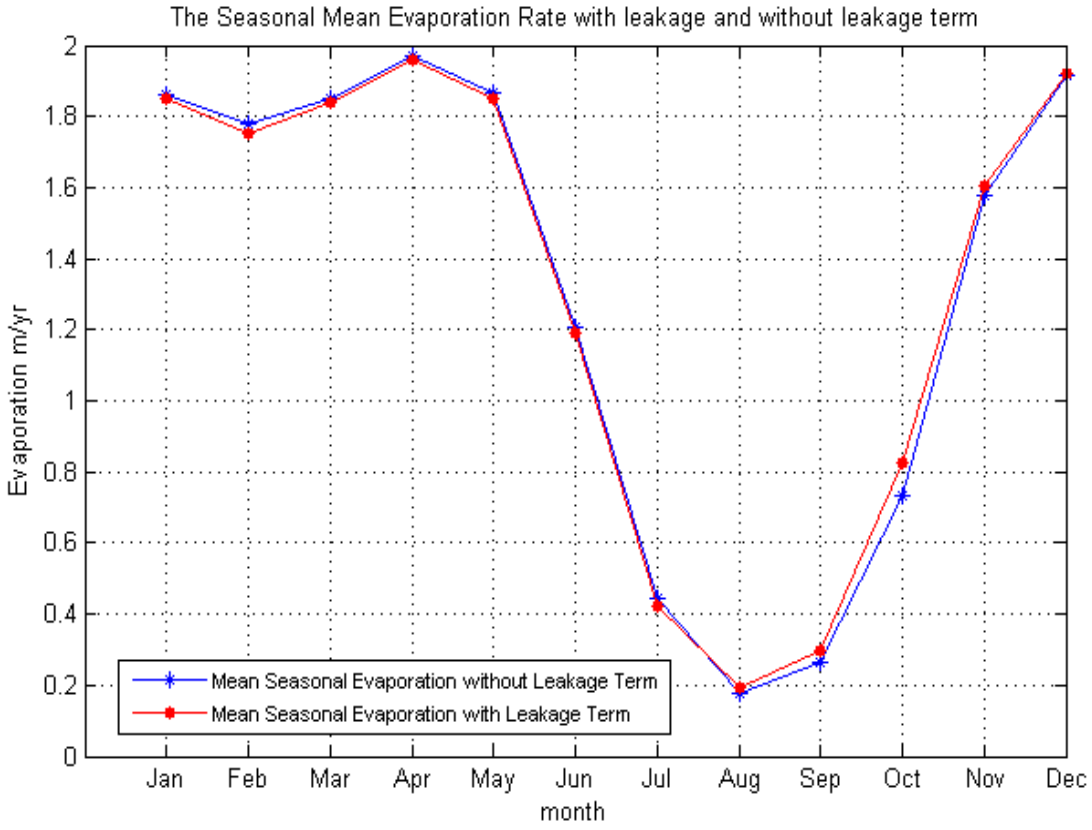

Figure 4.3: The seasonal mean net evaporation with leakage term and without leakage term

The net mean value of the evaporation with co-variances included is 1.31 m/yr. The difference between the red and the blue curve in Figure 4.4 presents the covariance of the anomalies from the annual mean of density, salinity, and current when calculating the net evaporation. The two curves show quite large differences for some years, for instance 1962, 1963, 1965 and 1969, which are the years of the largest differences. The figure also reveals that the covariance has usually small positive effect on the evaporation, but in some else years it is clear that the red curve is below the blue one thus, it has a negative effect for those years. Note also that the blue curve is the same as the curve shown in 4.1.

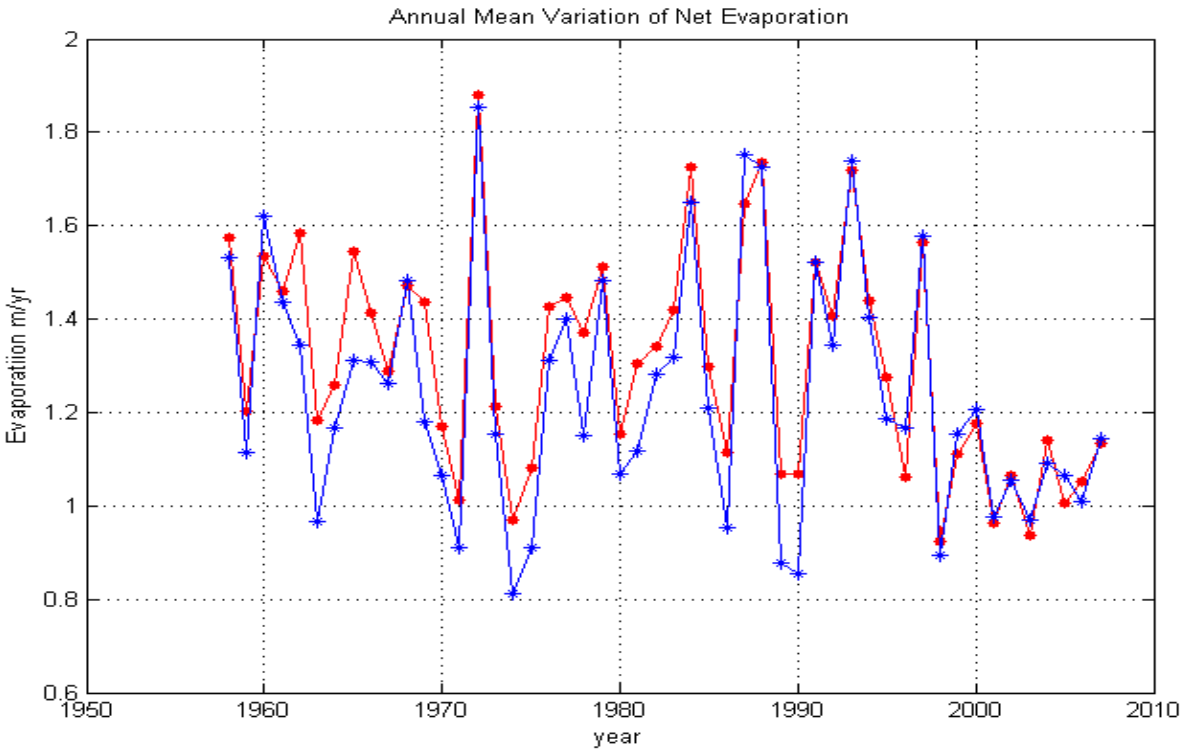

Figure 4.4: The annual mean variation of net evaporation. The blue curve is the annual mean of the component's product $\overline{psv}$, while the red curve is the product of the annual mean of the components $\bar{p}\bar{s}\bar{v}$.

Figure 4.5 presents the seasonal mean variation of the evaporation, and as in Figure 4.4 the curves show the mean of the component's product (blue curve), and the product of the component's means (red curve). It is clear that the co-variations are small, in contrast to the annual values shown in Figure 4.4. A closer look at the figure reveals that the co-variance has a positive effect on the evaporation in August, September and October, while it does not have that effect during other months. It has a small negative effect in February. This means that anomalies of for example June currents and salinities are not related, and hence do not contribute to the June mean evaporation, this means that the anomalies from the seasonal mean are not much correlated. The blue curve here is the same as the curve in Figure 4.2.

From Figures 4.2 and 4.5 it is clear that the effect of the co-variances is rather small for the seasonal variation that it just increased from 1.30 to 1.31 m/yr. For the interannual variation it is larger, there the mean value increased from 1.24 to 1.31 m/yr.

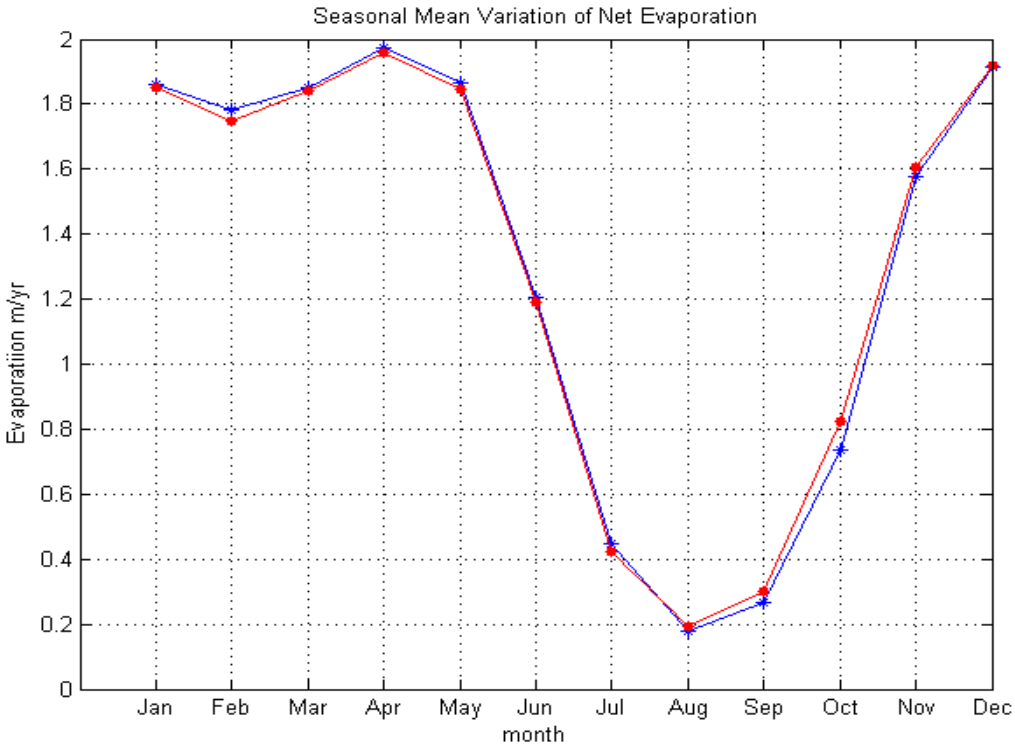

Figure 4.5: Seasonal Mean Variation of net evaporation. The blue curve is the monthly mean of the component's product $\overline{psv}$, while the red curve is the product of the monthly mean of the components $\bar{p}\bar{s}\bar{v}$.

The net evaporation estimates for each of the six hundred months from January 1958 to December 2007 (the blue*) are shown in Figure 4.6 together with the mean seasonal net evaporation (the red curve) plus and minus the standard deviation (the green curves). The minimum variance is in September, and the maximum one is in May month. The figure also reveals some negative values of the net evaporation in some summer months, and the largest negative value is close to -0.5 m/yr in July. It could be explained as the rate of the precipitation was higher than the rate of the evaporation during those months. Further reasons may be that the evaporation is hindered due to the high humidity and high static stability of the atmospheric surface layer during summer. But these obtained negative values may also be model artifacts.

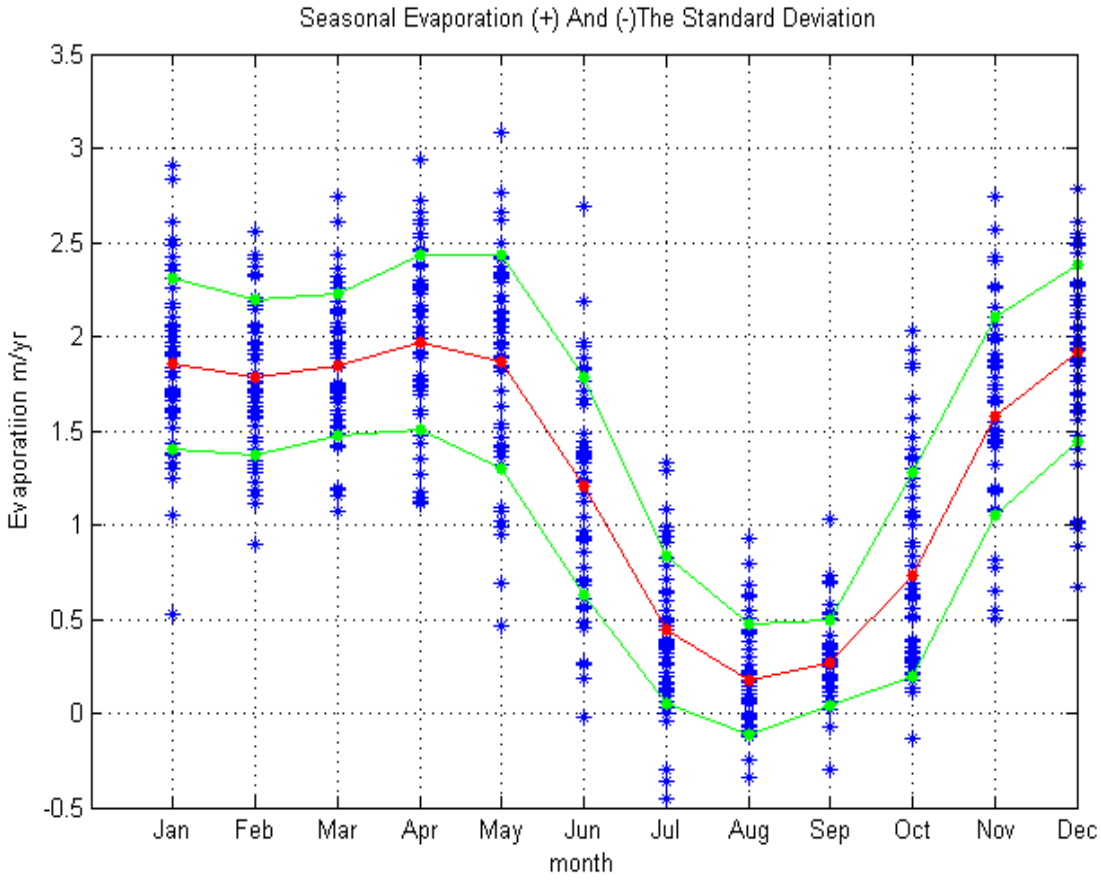

Figure 4.6: The seasonal net evaporation plus and minus the standard deviation. The blue asterisks denote the estimates for each single month.

4.2 Time Series of the Wind

Figures 4.7 and 4.8 present the seasonal mean eastward and northward wind stress at Hanish Sill respectively. The eastward wind stress changes its direction from being westward during October to May (winter), to being directed eastward during June to September. For the northward wind stress component it is interesting to note that it is positive at the sill throughout the whole year. The most notable thing is how weak the winds are there; a wind stress of 0.01Pa corresponds to a wind speed about 3 m s^{-1}.

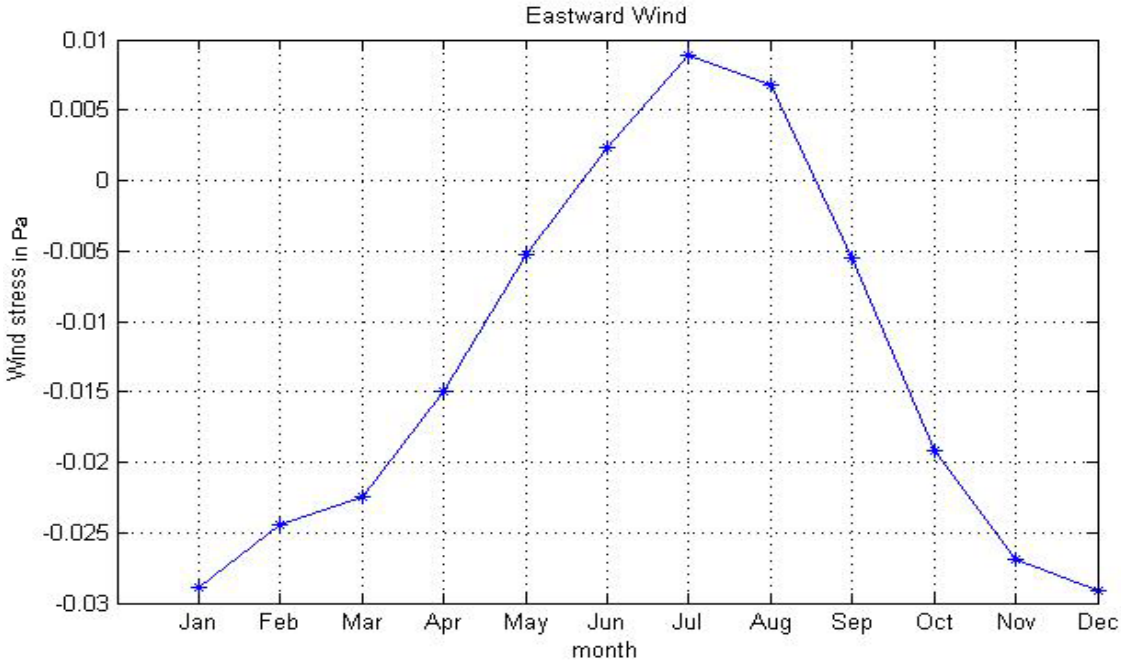

Figure 4.7: Seasonal mean eastward wind stress at Hanish Sill.

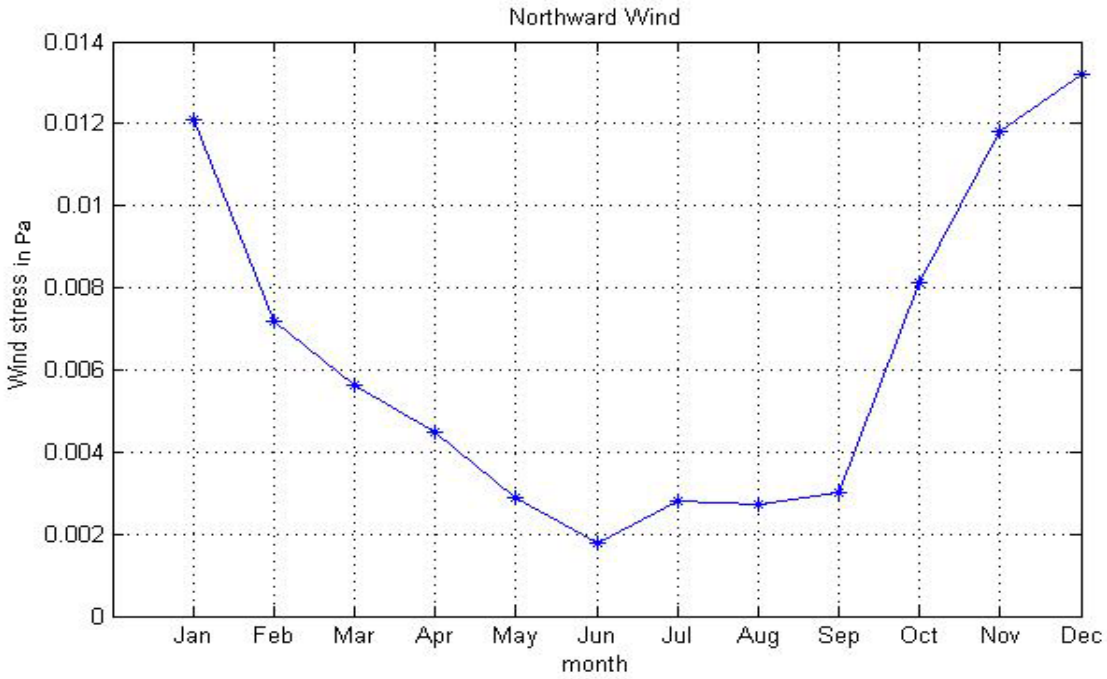

Figure 4.8: Seasonal mean northward wind stress at Hanish Sill.

The annual mean wind stress magnitude along the whole Red Sea during the period 1958 to 2007 is shown in Figure 4.9, the maximum value is in 2006 and the minimum is in 1965. There is not a clear relationship between the annual wind and the net annual evaporation rate. Their fluctuations are consistent for some years and inconsistent for other years. Also they are inconsistent in their magnitudes through the years even if they have fluctuated consistently. For instance the recent years 2003 – 2007 recorded a notable increase in wind magnitude whilst, Figure 4.1 showed a noticeable decrease in the net annual evaporation rate in the recent years, the year 1965 recorded the minimum magnitude of the wind while, the evaporation decreased in the same year, but it wasn't the minimum year recorded rate of the evaporation during the period of this study.

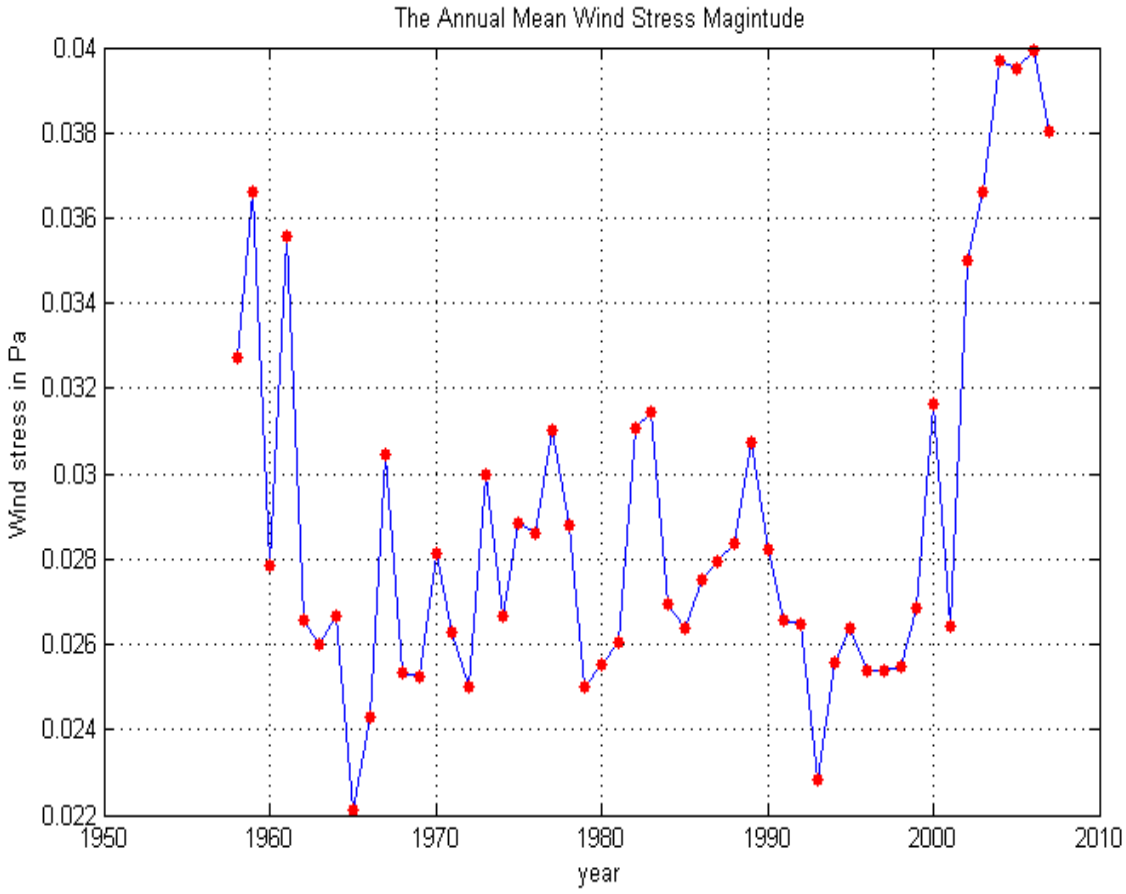

Figure 4.9: The Annual Mean Wind Stress Magnitude along the whole Red Sea.

Figure 4.10 shows the monthly mean wind stress magnitude averaged along the whole of the Red Sea. The wind increases from October and it gets its maximum value in February, then, it decreases in March, April and May before it increases a little again in June because of the summer monsoon. It is obvious from Figure 4.10 that the strong wind magnitudes were recorded during winter. There were some fluctuations during summer and autumn. The striking and most notable thing is the great difference between the winds magnitudes in February compared to May although evaporation is about the same! A careful examination of Figure 4.10 shows that the wind is feeble in April and May, despite the result of Figure 4.2 reveals a strong evaporation rates in the same months.

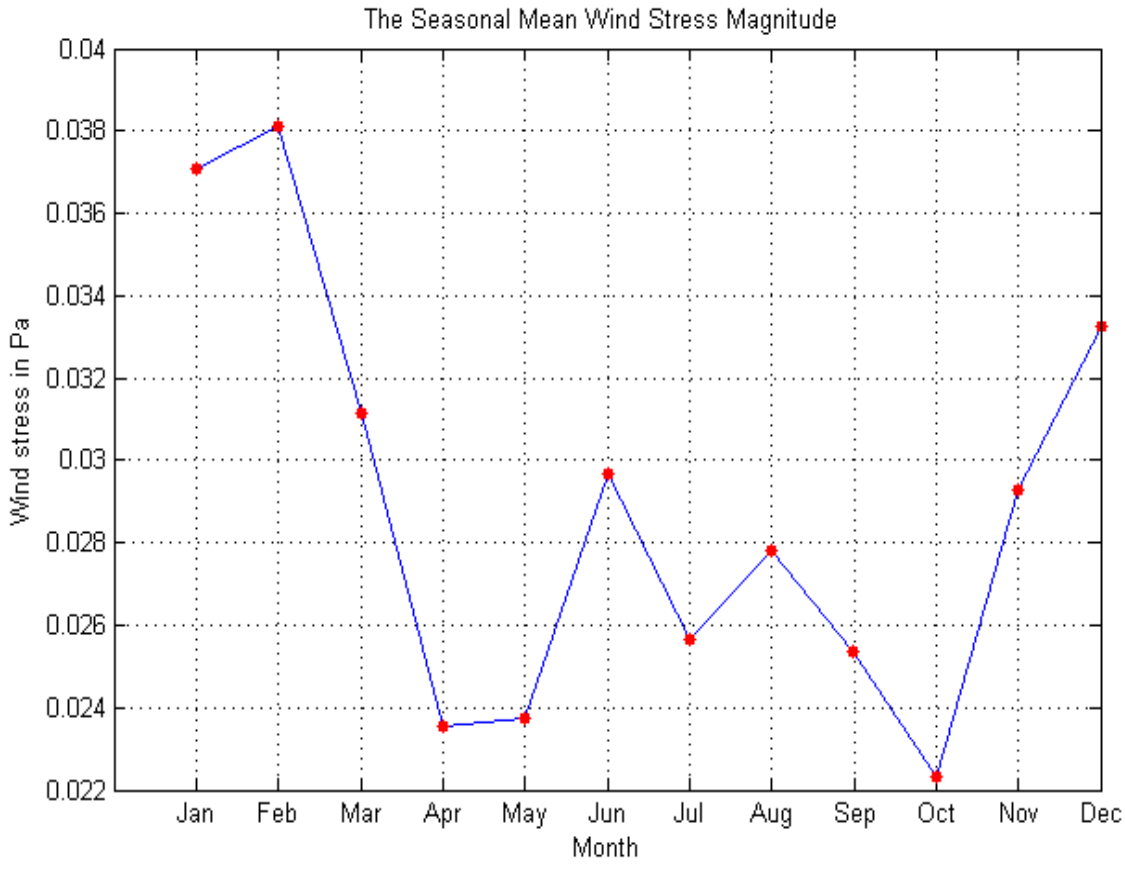

Figure 4.10: The Seasonal mean wind stress magnitude along the Red Sea.

4.3 The Flow Through Hanish Sill

The seasonal inflow and outflow in the Red Sea are displayed in Figure 4.11. The inflow (the blue curve)begins to increase from October and reaches its maximum volume in November and December (almost the same volume transports). It decreases a bit in February then, returns to increase again in March before it fluctuates and decreases a bit again in April. It clearly begins to decrease in May till it reaches its minimum value in August and September (almost equal values). The outflow (the red curve) behaves similarly. It increases from September to reach its maximum value in November and December then, there is a bit decrease in February before it increases again in March. The notable decrease begins in May and continues decreasing till it reaches its minimum volume transport in September. In other words Figure 4.11 reveals that the water flowing into the Red Sea from Gulf of Aden is greater during winter months (SE monsoon); than during autumn (NW monsoon); and this phenomenon has been explained by [21] and [26] as "because of the water loss caused by an increase in the rate of evaporation in the Red Sea" and could be consistent with our result that we found high evaporation rates during winter months. The figure also shows that the great difference between the Inflow and the Outflow found in the winter and the late winter months which are the same months when the high rate of the evaporation occurs (Figure 4.2). And also there are small differences between the Inflow and the Outflow in the summer months as the evaporation rate is small during the same season (Figure 4.2). There is approximately totally balanced flow in august (Inflow equal to Outflow); as the minimum rate of the evaporation is in August also (Figure 4.2). Hence, the aforementioned points are consistent with our assumption of that the difference between the Inflow and the Outflow assumed as the evaporated water.

The most marked thing when we make a comparison of Figure 4.11 to Figure 4.2 is the large evaporation in June compared to October in Figure 4.2 despite Figure 4.11 reveals that the water transport about the same in the two months!. If we take Figure 4.9 (mean seasonal wind magnitude) into account, the wind effect could give us an explanation for the question revealed from the previous comparison that the wind was relatively strong in June compared to October.

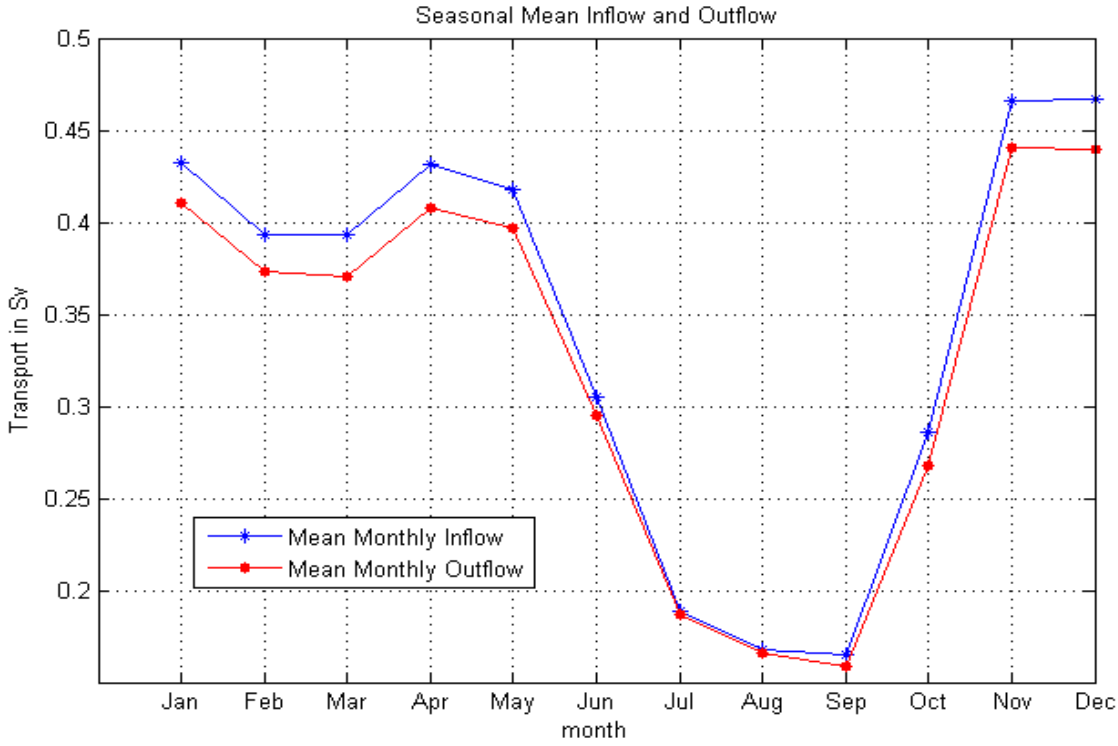

Figure 4.11: Seasonal Mean In and Outflow.

Figure 4.12 presents the relationship between the seasonal net evaporation and the seasonal Red Sea outflow (RSOW here is the deep water outflow); it shows a weak deep water outflow in summer months and this result is consistent with [31] and [23] who found a weak deep water outflow during the summer as a result of high winter evaporation in the north that raises the salinity and the density of the water there then, it sinks down and flows southward and forms outflow water in summer. The figure reveals also strong positive relation between the evaporation and the water outflow and that is expected according to the previous figures (Figures 4.2 and 4.11) which showed that the evaporation and water transport behaved in the same manner through the year. It is clear there should be a positive relationship between the evaporation and the inflow too.

There is a secondary minimum in RSOW in February which is also revealed by the evaporation. The wind stress has no such secondary minimum whether at Hanish Sill or averaged over the whole Red Sea. Actually the Red Sea average wind stress is at its maximum in February (Figure 4.10). This secondary minimum in RSOW is therefore clearly corresponding to the evaporation. This finding is also interesting in

the way that the February minimum marks a shift during the winter season. It hints at that there is a three-season division in the Red Sea: Summer-Early, Winter-Late and Winter.

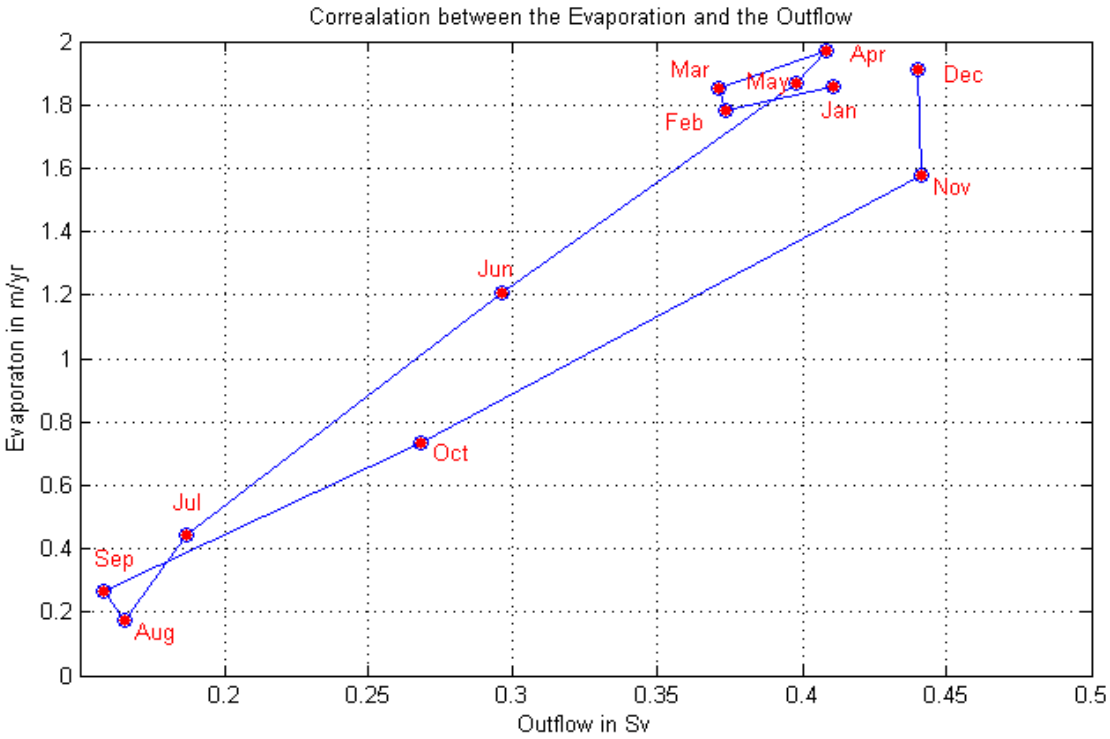

Figure 4.12: The relationship between net evaporation and outflow from the Red Sea.

Figure 4.13 is the same as Figure 4.12; but here it presents the relation between the seasonal mean evaporation and the seasonal water netflow (Inflow – Outflow). It is clear that there is a positive relation between the seasonal mean evaporation and the seasonal netflow as we calculated the evaporation rate based on this assumption of that the evaporated water is the seasonal differences between the inflow and the outflow as it aforementioned in Figure 4.11. The figure reveals high evaporation and high netflow during winter and low during summer with minimum value in August for both.

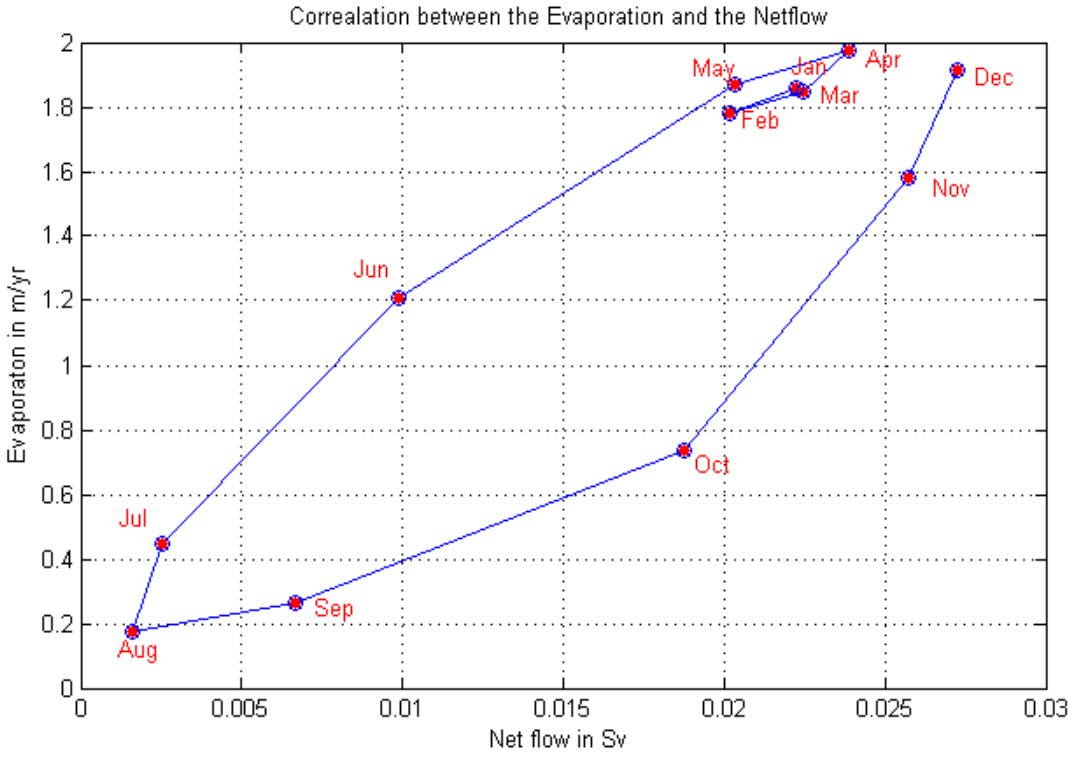

Figure 4.13: The Relationship between the Seasonal evaporation and the Seasonal Netflow (Netflow=Inflow-Outflow).

Chapter 5

Conclusion and Recommendations

5.1 Conclusion

The present study investigated the annual and seasona (monthly) mean net evaporation rate in the Red Sea during the period Jan 1958 – Dec 2007. The calculated net evaporation (E-P) is based on conservation of mass and salt of the Red Sea north of the Hanish sill (13.25°N) and by calculation of the fluxes of mass and salt across the sill. The results exhibit high variations of the annually and monthly mean net evaporation rate in the Red Sea.

The results reveal many interpretations consistent to some extent with previous estimations. For instance the results of monthly evaporation rates in the Red Sea as illustrated in Figure 4.2, it is clear that the greatest monthly evaporation rates are during winter months. This result is similar to and confirms Privett's [26] results, who also found that the evaporation is high duringwinter.

In their, Figure 8a, Tragou et al. [37] presented higher latent heat flux during winter than during summer (latent heat flux is proportional to the evaporation). Their results showed less seasonal variation than which is estimated in this study, as their summer values are more than half of the winter values, while the estimated summer values of this study are just about 20% of the winter values (after adding the estimated annual value of precipitation 0.15 myr^{-1}).

The annual mean net evaporation in this study estimated by 1.24 m yr^{-1}, is less; but can be considered as a comparable value to 1.54 myr^{-1} as estimated by Hastenrath and Lamb [13], 1.5 m yr^{-1} as estimated by da Silva et al. [10], and it is more than the value 1.1 m yr^{-1} Clifford et al. [8].

Throughout all the period, due to the evaporation, the inflow water enters into the Red Sea from Gulf of Aden showed wintertime maximums and summertime minimums. The seasonal transport through the sill was almost totally systematic with the seasonal evaporation oscillation therefore, we can suggest that evaporation exerts a great influence on the circulation of the Red Sea. There was a balance in the transport except in the winter when the large excess of the inflow over the outflow in the same months of the high evaporation rate which give a strong support to this work basic assumption that we calculated the rate of the evaporation based on assuming that the differences between the inflow and the outflow supposed to be the evaporated water.

There was a northward wind throughout the whole year at Hanish Sill. The summer prevailing winds at Hanish sill are claimed to be NNW although the SODA data rather show that they are WSW. As the evaporation, the monthly wind stress was strong during the winter months. The annual wind impact is masked, but it is clearer for the monthly, particularly in June and October when the water transport during these two months was about the same, but there was strong evaporation in June compared to the evaporation in October which can be explained as because of the wind stress was greater in June than October. Hence, the wind effect seems to be considerable in the aspect of seasonal instead of annual aspect. we can suggest that evaporation exerts a greater influence than the wind pattern on the circulation of the Red Sea.

Leakage term revealed small values, and it had a little effect on the calculated evaporation rates.

The advantage and the usefulness of the SODA model data is that it covers a long time period, and are regular in both time and space. They may therfore be used for budget calculations and studies of variations in the evaporation over sea areas like done here.

5.2 Recommendations

There are different relationships between the weather's and ocean's elements in aspects of air-sea interaction. All these factors affect each upon the others in a combined way. This makes it better to study all these factors once we try to estimate the behavior of a particular factor of them during a particular period.

In this study it would be better if we could obtain data of humidity, sea surface temperature (SST) and atmospheric pressure because these factors impact directly or indirectly in the evaporation rate. Also static stability of the atmospheric surface layer is an important parameter. Studying the behavior of these factors during the study period would reveal how they affected on the evaporation rates.

One of the weaknesses in our approach is the uncertainty of the model bathymetry of the SODA data so that we have been forced to calculate the bottom depth of Hanish sill. This also effects the calculation of the leakage terms in the mass and the salt balances. Hence, it would be good if the SODA data would include information on the sickness of the bottom cells.

Bibliography

[1] F. Ahmad and S.A.R. Sultan. On the heat balance terms in the central region of the Red Sea. *Deep Sea Research Part A. Oceanographic Research Papers*, 34 (10):1757–1760, 1987.

[2] F. Ahmed and S.A.R. Sultan. Surface heat fluxes and their comparison with the oceanic heat flow in the Red Sea. *Oceanologica acta*, 12(1):33–36, 1989.

[3] E.B. Ali. The Inorganic Carbon Cycle in the Red Sea. Master's thesis, Geophysical Institute, University of Bergen, Bergen, Norway, 2008.

[4] A.K. Bogdanova. Indirect estimation of the seasonal variation of the water exchange through Bab el Mandeb. *L'oceanographie physique de la Mer Rouge, CNEXO, Paris*, pages 253–265, 1974.

[5] A.F. Bunker, H. Charnock, and R.A. Goldsmith. A note on the heat balance of the Mediterranean and Red Seas. *Journal of Marine Research*, 40:73–84, 1982.

[6] J.A. Carton and B.S. Giese. A reanalysis of ocean climate using Simple Ocean Data Assimilation (SODA). *Monthly Weather Review*, 136(8):2999–3017, 2008.

[7] J.A. Carton, B.S. Giese, and S.A. Grodsky. Sea level rise and the warming of the oceans in the Simple Ocean Data Assimilation (SODA) ocean reanalysis. *Journal of Geophysical Research*, 110:C09006, 2005.

[8] M. Clifford, C. Horton, J. Schmitz, and L.H. Kantha. An oceanographic nowcast/forecast system for the Red Sea. *Journal of geophysical research*, 102(C11): 25101–25, 1997.

[9] J.R. Cochran. Red Sea. in AccessScience, ©McGraw-Hill Companies. Website visited 12 March 2012, 2008. http://www.accessscience.com/content.aspx?searchStr=red+sea&id=576200.

[10] A.M. da Silva, C.C. Young, and S. Levitus. Atlas of surface marine data 1994, Vol. 4: Anomalies of fresh water fluxes. *NOAA Atlas, NESDIS*, 9, 1994.

[11] F.W. Edwards. Climate and Oceanography. In A.J. Edwards and S.M. Head, editors, *The Red Sea*, pages 45–68. 1987.

[12] V. Güldal and H. Tongal. Cluster analysis in search of wind impacts on evaporation. *Applied Ecology and Environmental Research*, 6(4):69–76, 2008.

[13] S. Hastenrath and P.J. Lamb. *Climatic Atlas of the Indian Ocean, Part 2*, volume 19. University of Wisconsin Press, 1979.

[14] H. Jiang, J.T. Farrar, R.C. Beardsley, R. Chen, and C. Chen. Zonal surface wind jets across the Red Sea due to mountain gap forcing along both sides of the Red Sea. *Geophysical Research Letters*, 36:L19605, 2009. doi: 10.1029/2009GL040008.

[15] W.E. Johns, G.A. Jacobs, J.C. Kindle, S.P. Murray, and M. Carron. Arabian Marginal Seas and Gulfs. Technical Report 2000-01, University of Miami RSMAS, 1999.

[16] C. Maillard and G. Soliman. Hydrography of the Red Sea and exchanges with the Indian Ocean in summer. *Oceanologica Acta*, 9(3):249–269, 1986.

[17] *The Watershed ConceptMichigan Environmental Education Curriculum*. The Watershed Concept. Website visited 5 February, 2012. http://techalive.mtu.edu/meec/module01/EvaporationandTranspiration.htm.

[18] S.A. Morcos. Physical and chemical oceanography of the Red Sea. *Oceanography and Marine Biology: An Annual Review*, 8:73–202, 1970.

[19] S.P. Murray and W. Johns. Direct observations of seasonal exchange through the Bab el Mandab Strait. *Geophysical Research Letters*, 24(21):2557–2560, 1997.

[20] A.C. Neumann and D.A. McGill. Circulation of the Red Sea in early summer. *Deep Sea Research (1953)*, 8(3-4):223–235, 1961.

[21] J. Neumann. Evaporation from the Red Sea. *Israel Exploration Journal*, 2(3): 153–162, 1952.

[22] M.M. Osman. Evaporation from coastal water off Port-Sudan. *Journal of the Faculty of Marine Science (Jeddah)*, 4:29–37, 1985.

[23] W.C. Patzert. Wind-induced reversal in Red Sea circulation. In *Deep Sea Research and Oceanographic Abstracts*, volume 21, pages 109–121. Elsevier, 1974.

[24] W.C. Patzert. Volume and heat transports between the red sea and the gulf of aden, and notes on the red sea heat budget. In *International Association of Physical Science Ocean (IAPSO) Symposium Physical Oceanography of the Red Sea SCOR and UNESCO, Paris*, number 2, pages 191–201, 1974.

[25] D.E. Pedgley. An outline of the weather and climate of the Red Sea. *L´Oceanographie Physique de la Mer Rouge*, pages 9–27, 1974.

[26] D.W. Privett. Monthly charts of evaporation from the N. Indian Ocean (including the Red Sea and the Persian Gulf). *Quarterly Journal of the Royal Meteorological Society*, 85(366):424–428, 1959.

[27] Red Sea. Encyclopædia Britannica Online. Website visited 12 March, 2012. http://www.britannica.com/EBchecked/topic/494479/Red-Sea.

[28] Red Sea. Inc. Wikimedia Foundation. Website visited 12 March, 2012. http://en.wikipedia.org/wiki/Red_Sea#cite_note-1.

[29] Red Sea. Inc. Wikimedia Foundation. Website visited 11 March, 2012. http://http://en.wikipedia.org/wiki/Red_Sea#Oceanography.

[30] G. Siedler. General circulation of water masses in the Red Sea. In E.T. Degens and D.A. Ross, editors, *Hot Brines and Recent Heavy Metal Deposits in the Red Sea*, pages 131–137. Springer-Verlag, New York, 1969.

[31] D.A. Smeed. Exchange through the Bab el Mandab. *Deep Sea Research Part II: Topical Studies in Oceanography*, 51(4-5):455–474, 2004.

[32] S.S. Sofianos and W.E. Johns. An Oceanic General Circulation Model (OGCM) investigation of the Red Sea circulation: 2. Three-dimensional circulation in the Red Sea. *Journal of Geophysics Research*, 108:3066–3080, 2003.

[33] S.S. Sofianos, W.E. Johns, and S.P. Murray. Heat and freshwater budgets in the Red Sea from direct observations at Bab el Mandeb. *Deep Sea Research Part II: Topical Studies in Oceanography*, 49(7-8):1323–1340, 2002.

[34] SA Sultan, F. Ahmad, and A. El-Hassan. Seasonal variations of the sea level in the central part of the Red Sea. *Estuarine, Coastal and Shelf Science*, 40(1):1–8, 1995.

[35] E.F. Thompson. Chemical and Physical Investigations: the Exchange of Water Between the Red Sea and the Gulf of Aden Over the Sill. Technical Report 1933-34, Order of the Trustees of the British Museum, 1939.

[36] M. Tomczak and J.S. Godfrey. Regional Oceanography: An Introduction, 2003.

[37] E. Tragou, C. Garrett, R. Outerbridge, and C. Gilman. The heat and freshwater budgets of the Red Sea. *Journal of physical oceanography*, 29(10):2504–2522, 1999.

[38] UNEP. Assessment of Land-based Sources and Activities Affecting the Marine Environment in the Red Sea and Gulf of Aden, 1997.

[39] F. Vercelli. RicherchedioceanografiafisicaeseguitedellaR. Nave AmmiraglioMagnaghi (1923–1924). Part I. Correnti e maree. *Annali Idrografici*, 11:1–188, 2002.

[40] vtaide.com. Factors affecting the rate of evaporation. Website visited 15 February, 2012. http://www.vtaide.com/png/evaporation.htm.

[41] F. Werner and K. Lange. A bathymetric survey of the Sill Area between the Red Sea and the Gulf of Aden. *Geologisches Jahrbuch D*, 13:125–130, 1975.

[42] G. Wüst. Gesetzmäßige wechselbeziehungen zwischen ozean und atmosphäre in der zonalen verteilung von oberflächensalzgehalt, verdunstung und niederschlag. *Meteorology and Atmospheric Physics*, 7(1):305–328, 1954.

[43] N.I. Yegorov. Calculation of the heat balance of the Red Sea. *Meteorologiya i Gidrologiya*, 3:49–56, 1950.

[44] L. Yu. Global variations in oceanic evaporation (1958-2005): The role of the changing wind speed. *Journal of climate*, 20(21):5376–5390, 2007.